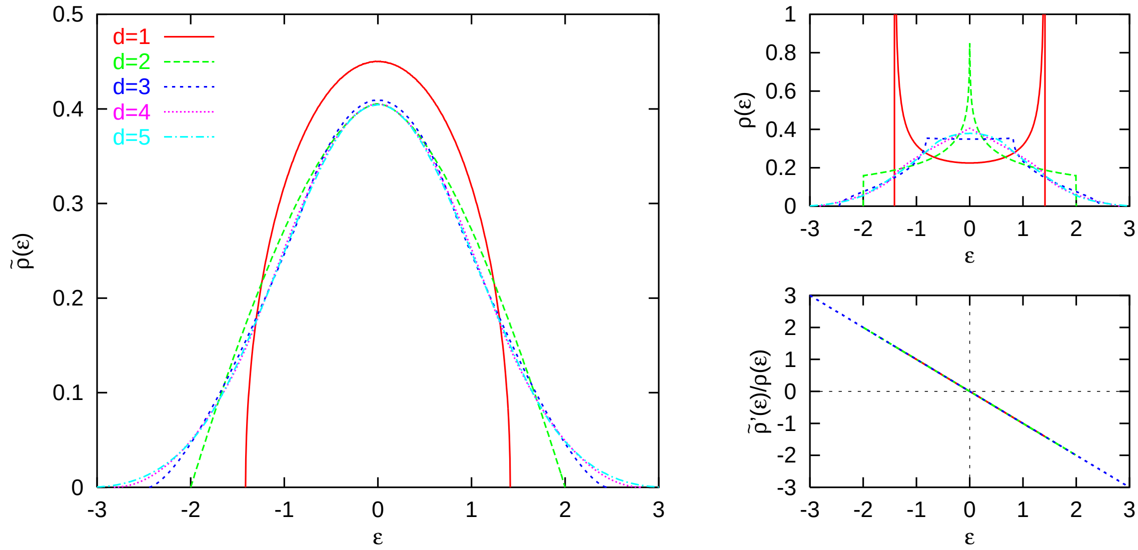

Figure 4.18: DMFT transport characteristics of the hypercubic (hc) lattice with NN hopping (cf. Fig. 4.14). The approach of the limiting Gaussian form (for $d \to \infty$) is much faster for $\tilde{\rho}(\epsilon)$ than for the DOS $\rho(\epsilon)$. The exact relation $\tilde{\rho}'(\epsilon)/\rho(\epsilon) = -\epsilon$ implies the proportionality of the f-sum to the kinetic energy.

described by (4.139) leads to $v^2_{\boldsymbol{k},x} = 2d{t'_{\parallel}}^2 {\epsilon^{hc}_{\boldsymbol{k}}}^2$. If the hyperplanes are, e.g., hypercubic, we get $\langle v^2_{\boldsymbol{k},x}\rangle(\epsilon) = 2d{t'_{\parallel}}^2\epsilon^2$. In contrast, if the hyperplanes are also of the fcc-type with $t'_{\perp} = t'_{\parallel} = \frac{t'^{*}}{\sqrt{2d(d-1)}}$, the resulting expression is $\langle v^2_{\boldsymbol{k},x}\rangle(\epsilon) = 2\frac{t'^{*2}}{d}(1 + \frac{\sqrt{2}}{t'^{*}}\epsilon)$. In the latter case we find that the squared Fermi velocity vanishes at the band edge as always for isotropic systems.

4.5.2 Optical Conductivity in Finite Dimensions

In this subsection we continue the discussion of transport related lattice properties in finite dimensions for a series of commonly treated lattice types. With the exception of the dimension-independent analytic forms for $\tilde{\rho}'(\epsilon)/\rho(\epsilon)$ available for the hc and fcc cases, all curves have been obtained by Monte Carlo sampling of the appropriate $\boldsymbol{k}$-space expressions. Apart from possible uses of this data as input for computations of $\sigma(\omega)$ in a local theory in finite dimensions, the study is also useful as support for the results of the general-dispersion method which may be used as a black-box algorithm for generating $\tilde{\rho}(\epsilon)$ from the noninteracting DOS $\rho(\epsilon)$ alone.

Fig. 4.18 shows that $\tilde{\rho}(\epsilon)$ converges much faster to its Gaussian $d = \infty$ form than the DOS on the hc lattice. This is possible since van-Hove singularities appearing in the DOS are cancelled by corresponding dips in the squared Fermi velocity. As visualized in Fig. 4.19 a, the Fermi velocity becomes more and more effectively constant and approaches unity for $d \to \infty$. In Fig. 4.19 b corresponding curves are shown for the fcc lattice which approach a tilted straight line vanishing at the band edge for